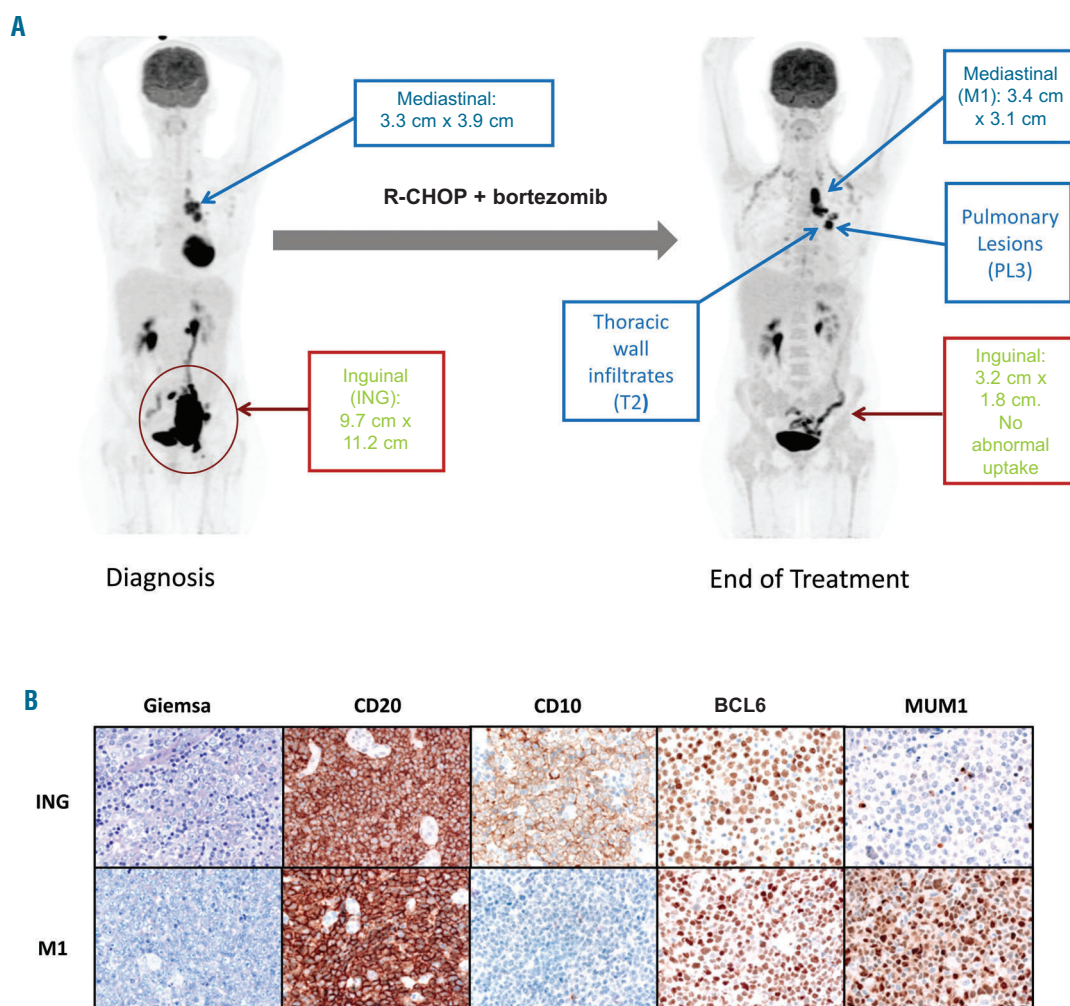


**Genetic heterogeneity highlighted by differential FDG-PET response in diffuse large B-cell lymphoma**

Intratumor heterogeneity (ITH) has emerged as a key theme to understanding the mechanisms driving treatment failure and relapse. Studies in many different cancers have revealed varying degrees of molecular heterogeneity both within and between biopsies taken from different sites of disease in the same patient.<sup>1</sup> In practice, the rarity of multi-site sampling in diffuse large B-cell lymphoma (DLBCL) has restricted studies to single biopsies at the time of diagnosis and these have been highly informative in characterizing unique molecular subtypes, based on the gene expression-derived cell-of-origin (COO) (activated B-cell [ABC], germinal center B-cell [GCB])<sup>2</sup> or distinct molecular subgroups that demonstrate a differential response to immuno-chemotherapy.<sup>3,4</sup> In this study we had an opportunity to examine both spatial and temporal heterogeneity, performing whole exome

sequencing on four tumors from the same patient that demonstrated a discordant response to immuno-chemotherapy, providing a unique insight into the relationship between ITH and treatment response.

A 50-year-old female presented with rapidly growing lymphadenopathy including a left inguinal mass (9.7x11.2 cm) and a left mediastinal mass (3.9x3.3 cm) without organomegaly or B-symptoms (Figure 1A). An inguinal biopsy (ING) revealed the diagnosis of DLBCL and imaging showed stage III disease with an International Prognostic Index (IPI) score of 2 (raised lactate dehydrogenase [LDH] 349 U/L). Immunohistochemical staining of the inguinal biopsy demonstrated; CD10<sup>+</sup>, BCL6<sup>+</sup> and MUM1<sup>-</sup> disease; consistent with GCB classification according to Hans' criteria<sup>8</sup> (Figure 1B). The patient was enrolled into the REMoDL-B trial<sup>9</sup> and randomized to the experimental arm with R-CHOP (rituximab, cyclophosphamide, doxorubicin, vincristine and prednisolone) and bortezomib from the second cycle. After six cycles of treatment, a



**Figure 1. Response to treatment and histologic findings.** (A) Positron emission tomography scan demonstrating the sites of disease at diagnosis and after six cycles of RCHOP and bortezomib chemotherapy. The biopsies profiled include the diagnostic inguinal biopsy (ING), and the treatment-refractory M1, thoracic wall (T2) and pulmonary lesions (PL3). (B) Representative histologic and Immunohistochemistry (IHC) images demonstrating DLBCL in the ING and mediastinal (M1). All images are shown at the original magnification of x400. Both tumors express CD20, while the ING tumor is positive for CD10, BCL6 and negative for MUM1 and the M1 biopsy is negative for CD10 and positive for BCL6 and MUM1. The Hans cell-of-origin classification<sup>8</sup> for the ING biopsy is GCB DLBCL and the M1 biopsy is non-GCB DLBCL, in keeping with the classification using the gene expression-based assay, Lymph2Cx. R-CHOP: rituximab, cyclophosphamide, doxorubicin, vincristine and prednisolone; GCB: germinal center B-cell; DLBCL: diffuse large B-cell lymphoma.

positron emission tomography-computed tomography (PET-CT) scan revealed complete metabolic response of the inguinal node but persistence of and the development of additional lesions above the diaphragm, consistent with progressive metabolic disease. At this time, biopsies were collected at three sites; mediastinal (M1), thoracic wall (T2) and pleural (PL3) confirming the progression of DLBCL. Immunohistochemical staining of the mediastinal biopsy demonstrated; CD10<sup>-</sup>, BCL6<sup>+</sup>, MUM1<sup>+</sup> disease, which was discordant with the inguinal biopsy, with the COO reported as non-GCB type according to Hans' criteria<sup>8</sup> (Figure 1B). Fluorescence *in situ* hybridization (FISH) analysis for *MYC*, *BCL2* and *BCL6* rearrangements were negative in all samples. The patient was

treated with salvage chemotherapy (rituximab, ifosfamide, carboplatin, etoposide) to a partial response followed by an autologous stem cell transplant but after an initial response experienced progressive disease and died two years from her initial diagnosis.

We next performed in-depth molecular profiling to determine whether the observed clinical heterogeneity was mirrored by molecular ITH. The COO was assessed using the Lymph2Cx assay,<sup>5</sup> with the inguinal biopsy classified as GCB and the chemo-refractory sites above the diaphragm as either ABC (M1) or unclassified (T2, PL3). Whole exome sequencing was performed on all four biopsies and germline material obtained from uninvolved bone marrow (mean coverage of 67x) (*Online*

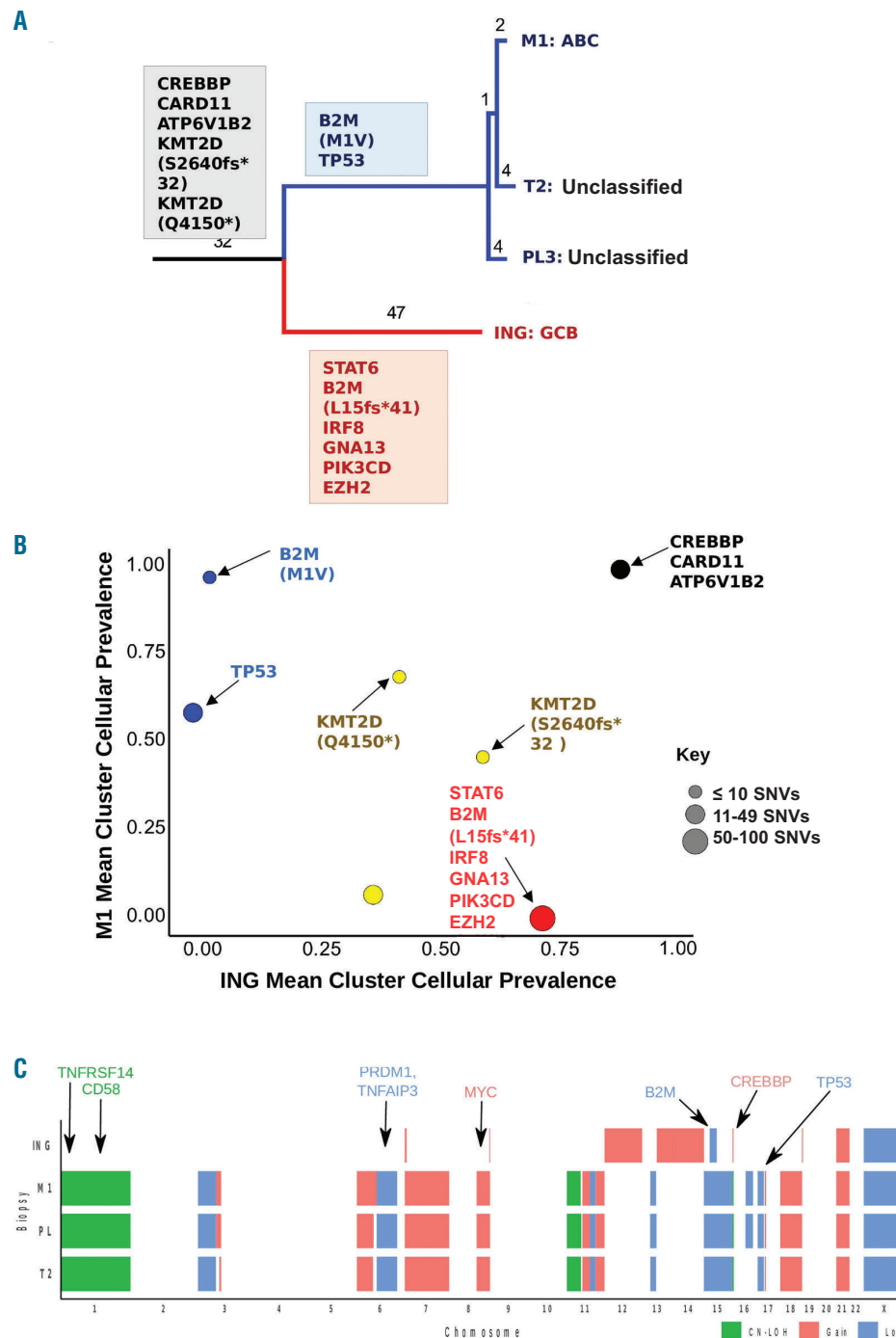


**Figure 2. The shared and discordant genetic changes between the different tumor sites profiled.** (A) Phylogenetic tree generated from non-synonymous and synonymous mutations in the samples sequenced. The number of mutations in each branch of the phylogenetic tree are shown. The chemo-sensitive inguinal biopsy (red) and three chemo-resistant biopsies (blue) above the diaphragm diverge early and evolve separately acquiring distinct secondary mutations. Shared mutations are shown in black. Site-specific mutations are shown in blue and red. The cell-of-origin (COO) classification using the Lymph2Cx assay is shown for each biopsy. (B) Pairwise mean cluster cellular prevalence (MCCP) plot of inguinal (ING) biopsy versus mediastinal (M1) biopsy. Derived mutation clusters represent the mean cellular prevalence of all mutations within a cluster. Each cluster is denoted by a circle with the size of the circle equivalent to the number of mutations within a cluster. The major clone is shown in black, shared subclones in yellow and site specific clones in red (ING) and blue (M1). Mutations in known DLBCL-associated genes are highlighted to show their locations within clusters. Additional MCCP plots are shown in the *Online Supplementary Figure S1*. (C) Copy number loss of heterozygosity (CNLOH; green), amplifications (red) and deletions (blue) are shown for each biopsy, demonstrating greatest genetic discordance between the ING biopsy (ING) and disease above the diaphragm (M1, T2, PL3). Genes of interest, mapped from UCSC Genome Browser (GRCh37/hg19) are highlighted. ^The loci harboring *CREBBP* demonstrates CNLOH in M1, T2, PL3 and copy number gain in ING.

*Supplementary Materials and Methods*).<sup>6</sup> The tumor purity was predicted across samples using the mclust algorithm and PyClone, a model-based clustering algorithm, was used to derive pairwise sub(clonal) clusters between each combination of biopsies (*Online Supplementary Materials and Methods*).<sup>7</sup>

The mutational profile between all four biopsies revealed significant differences between the inguinal biopsy and all three sites of supra-diaphragmatic disease. A total of 17 non-synonymous variants were shared across all four samples and included mutations in *CREBBP* (p.R1446C), *KMT2D* (p.Q4150\* and p.S2640fs\*32), and *CARD11* (p.M360V) (Figure 2A). These shared mutations represent early pathogenic events, occurring before marked evolutionary divergence, reminiscent of phylogenetic studies performed in follicular lymphoma and provide genetic evidence for a common progenitor cell (CPC) pool of B cells, responsible for the emergence of new clonal populations of disease.<sup>10,11</sup> Thirty-six non-synonymous variants were unique to the inguinal biopsy with a high level of genetic semblance observed between the three thoracic samples (M1, T2, PL3) (Figure 2A).

The mutational profile of the inguinal biopsy was consistent with the GCB subtype, demonstrating mutations in *EZH2* (p.Y646N), *STAT6* (p.E372K), and *GNA13* (p.L244P). Both the GCB subtype and mutations in *EZH2* are associated with apparent good risk disease and reflect this clinical scenario with the inguinal biopsy responding to treatment. In contrast, all the chemo-refractory biopsies above the diaphragm (M1, T2, PL3) shared a mutation and copy number loss in *TP53*, linked with an adverse outcome in DLBCL, and resistance to standard immuno-chemotherapy approaches. Additional alterations in M1, T2 and PL3 associated with the ABC subtype included copy number losses in *PRDM1* and *TNFAIP3*, genes involved in plasma cell differentiation and NFκB signaling, respectively. There was also evidence of convergent evolution, with different mutations and copy number losses detected at the *B2M* locus, in the inguinal (p.L15fs\*41) (ING) and thoracic biopsies (p.M1V), (M1, T2, PL3) (Figure 2A-C). Both genetic lesions are predicted to result in disruption of the major histocompatibility complex (MHC) Class I machinery and antigen presentation consistent with a selection pressure to acquire mechanisms of immune escape, reflecting recent studies demonstrating a diverse range of genetic lesions leading to immune evasion in the majority of DLBCL tumors.<sup>12</sup>

To reconstruct the clonal substructure of these spatially separated tumors, mean cluster cellular prevalence (MCCP) plots were generated for each pairwise combination of biopsies (*Online Supplementary Materials and Methods*) and replicated the same pattern of ITH (*Online Supplementary Figure S1*). The greatest genetic divergence, demonstrated by the non-linear distribution of subclones, was between the inguinal and three supra-diaphragmatic biopsies (Figure 2B). A comparison of the shared variants between all four biopsies uncovered differences in clonality, with the *CREBBP* mutation (p.R1446C) representing a clonal mutation, whilst the shared *KMT2D* mutations (p.Q4150\* and p.S2640fs\*32), arose in distinct subclones. Collectively, the phylogenetic reconstruction and MCCP plots offer compelling evidence that the inguinal biopsy and three thoracic samples diverged early from an ancestral clone (CPC), which harbored the *CREBBP* mutation and evolved separately into markedly different genetic and COO subtypes. Since

biopsies were not available from the mediastinal disease at diagnosis, it is not possible to say exactly when this evolutionary divergence arose, however temporal profiling studies and a recent example of donor-derived DLBCL<sup>13,14</sup> all point to a CPC-like population in a subset of cases which contributes to the tumor's ability to evolve and evade treatment.

Patients with refractory disease occur in up to 20% of cases, are seldom re-biopsied and experience extremely poor outcomes, indicating a significant unmet need.<sup>15</sup> In this case we were able to describe the extent of genetic ITH between the chemo-sensitive and chemo-refractory sites of disease and highlight the potential pitfalls when classifying tumors based on a single biopsy, an area of increasing relevance as further refinements to the molecular classification of DLBCL are made.<sup>3-4,16</sup> To better assess the frequency and consequences of increased ITH and its role as a prognostic biomarker in these difficult to treat subsets of patients, studies incorporating multi-site biopsies and molecular profiling of refractory lesions identified by imaging coupled with cell-free tumor DNA analyses should be considered.<sup>17</sup>

Shamzah Araf,<sup>1</sup> Koorosh Korfi,<sup>1</sup> Findlay Bewicke-Copley,<sup>1,2</sup> Jun Wang,<sup>2</sup> Sergio Cogliatti,<sup>3</sup> Emil Kumar,<sup>1</sup> Flavio Forrer,<sup>4</sup> Sally F. Barrington,<sup>5</sup> Trevor A. Graham,<sup>6</sup> David W. Scott,<sup>7</sup> Lisa M. Rimsza,<sup>8</sup> Andrew Davies,<sup>9</sup> Peter Johnson,<sup>9</sup> Jessica Okosun,<sup>1</sup> Jude Fitzgibbon<sup>10</sup> and Martin Fehr<sup>10\*</sup>

\*JF and MF contributed equally as co-senior authors.

<sup>1</sup>Centre for Haemato-Oncology, Barts Cancer Institute, Queen Mary University of London, London, UK; <sup>2</sup>Centre for Molecular Oncology, Barts Cancer Institute, Queen Mary University of London, London, UK; <sup>3</sup>Institute of Pathology, Cantonal Hospital St Gallen, St Gallen, Switzerland; <sup>4</sup>Department of Nuclear Medicine, Cantonal Hospital St Gallen, St Gallen, Switzerland; <sup>5</sup>King's College London and Guy's and St Thomas' PET Centre, School of Biomedical Engineering and Imaging Sciences, King's College London, King's Health Partners, London, UK; <sup>6</sup>Evolution and Cancer Laboratory, Barts Cancer Institute, Queen Mary University of London, London, UK; <sup>7</sup>Centre for Lymphoid Cancer, British Columbia Cancer Agency, Vancouver, BC, Canada; <sup>8</sup>Department of Laboratory Medicine and Pathology, Mayo Clinic, Scottsdale, AZ, USA; <sup>9</sup>Cancer Research UK Centre, University of Southampton, Southampton, UK and <sup>10</sup>Clinic for Medical Oncology and Haematology, Cantonal Hospital St Gallen, St Gallen, Switzerland

*Funding:* this work was supported by grants from Cancer Research UK (15968 awarded to JF, Clinical Research Fellowship awarded to SA) and Bloodwise through funding of the Precision Medicine for Aggressive Lymphoma (PMAL) consortium (15002). SFB acknowledges support from the National Institute for Health Research and Social Care (NIHR) [RP-2-16-07-001]. King's College London and UCL Comprehensive Cancer Imaging Centre is funded by the CRUK and EPSRC in association with the MRC and Department of Health and Social Care (England). The views expressed are those of the author(s) and not necessarily those of the NHS, the NIHR or the Department of Health and Social Care.

*Correspondence:*

SHAMZAH ARAF - s.araf@qmul.ac.uk  
JUDE FITZGIBBON - j.fitzgibbon@qmul.ac.uk  
doi:10.3324/haematol.2019.242206

*Information on authorship, contributions, and financial & other disclosures was provided by the authors and is available with the online version of this article at [www.haematologica.org](http://www.haematologica.org).*

## References

- McGranahan N, Swanton C. Clonal heterogeneity and tumor evolution: past, present, and the future. *Cell*. 2017;168(4):613-628.

2. Alizadeh AA, Eisen MB, Davis RE, et al. Distinct types of diffuse large B-cell lymphoma identified by gene expression profiling. *Nature*. 2000;403(6769):503-511.
3. Chapuy B, Stewart C, Dunford AJ, et al. Molecular subtypes of diffuse large B cell lymphoma are associated with distinct pathogenic mechanisms and outcomes. *Nat Med*. 2018;24(5):679-690.
4. Schmitz R, Wright GW, Huang DW, et al. Genetics and pathogenesis of diffuse large B-cell lymphoma. *N Engl J Med*. 2018;378(15):1396-1407.
5. Scott DW, Wright GW, Williams PM, et al. Determining cell-of-origin subtypes of diffuse large B-cell lymphoma using gene expression in formalin-fixed paraffin-embedded tissue. *Blood*. 2014;123(8):1214-1217.
6. Araf S, Wang J, Korfi K, et al. Genomic profiling reveals spatial intratumor heterogeneity in follicular lymphoma. *Leukemia*. 2018;32(5):1261-1265.
7. Roth A, Khattra J, Yap D, et al. PyClone: statistical inference of clonal population structure in cancer. *Nat Methods*. 2014;11(4):396-398.
8. Hans CP, Weisenburger DD, Greiner TC, et al. Confirmation of the molecular classification of diffuse large B-cell lymphoma by immunohistochemistry using a tissue microarray. *Blood*. 2004;103(1):275-282.
9. Davies A, Cummin TE, Barrans S, et al. Gene-expression profiling of bortezomib added to standard chemoimmunotherapy for diffuse large B-cell lymphoma (REMoDL-B): an open-label, randomised, phase 3 trial. *Lancet Oncol*. 2019;20(5):649-662.
10. Green MR, Gentles AJ, Nair RV, et al. Hierarchy in somatic mutations arising during genomic evolution and progression of follicular lymphoma. *Blood*. 2013;121(9):1604-1611.
11. Okosun J, Bödör C, Wang J, et al. Integrated genomic analysis identifies recurrent mutations and evolution patterns driving the initiation and progression of follicular lymphoma. *Nat Genet*. 2014;46(2):176-181.
12. Challa-Malladi M, Lieu YK, Califano O, et al. Combined genetic inactivation of  $\beta$ 2-Microglobulin and CD58 reveals frequent escape from immune recognition in diffuse large B cell lymphoma. *Cancer Cell*. 2011;20(6):728-740.
13. Araf S, Wang J, Ashton-Key M, et al. Transmission of diffuse large B-cell lymphoma by an allogeneic stem-cell transplant. *Haematologica*. 2019;104(4):e174-e177.
14. Juskevicius D, Lorber T, Gsponer J, et al. Distinct genetic evolution patterns of relapsing diffuse large B-cell lymphoma revealed by genome-wide copy number aberration and targeted sequencing analysis. *Leukemia*. 2016;30(12):2385-2395.
15. Crump M, Neelapu SS, Farooq U, et al. Outcomes in refractory diffuse large B-cell lymphoma: results from the international SCHOLAR-1 study. *Blood*. 2017;130(16):1800-1808.
16. Reddy A, Zhang J, Davis NS, et al. Genetic and functional drivers of diffuse large B Cell lymphoma. *Cell*. 2017;171(2):481-494.
17. Bohers E, Vially PJ, Becker S, et al. Non-invasive monitoring of diffuse large B-cell lymphoma by cell-free DNA high-throughput targeted sequencing: analysis of a prospective cohort. *Blood Cancer J*. 2018;8(8):74.